

A novel non-linear model for multilayer rubber bearing isolators with load interaction

N.E. Maureira

Department of Civil Engineering, Universidad Católica de la Santísima Concepción, Concepción, Chile.

PhD. Candidate, Pontificia Universidad Católica de Chile, Santiago, Chile.



2014 NZSEE
Conference

ABSTRACT: A novel non-linear mathematical model is proposed to characterize the mechanical behaviour of a circular elastomeric rubber isolator. This model considers the geometric non-linearities due to large deformations. It represents the coupling between the axial and shear loads, with the corresponding vertical and lateral displacements, including the loss of axial and lateral stiffness in the isolator generated by excessive lateral displacements and compression. This model is also capable of characterizing the isolator behaviour under tensile loads and its effect on the lateral stiffness.

This is an upgrade of an existing model for elastomeric isolators that only characterize the relationship between the axial and shear forces, and the corresponding vertical and lateral displacements. The proposed model is also able to characterize the internal strain-stress state in any rubber sheet.

From the results of the model proposed, it is concluded that the buckling load is higher under tensile loads than under compression, whereas the behaviour of the isolator is non-symmetric with respect to the axial load. Furthermore, when considering an axial load magnitude lower than 10% of the buckling load in compression, the difference between the behaviour of the maximum normal stress and strain as a function of axial load and lateral displacement, is substantially different under tension in comparison with compression. It is shown by an example that lateral displacements of around $\pm 40\%$ of the isolator's radius and axial tensile loads up to 10% of buckling load are allowed without cavitation in the rubber.

1 INTRODUCTION

One of the most used techniques in the world for seismic protection of buildings is seismic isolation, being the circular multilayer elastomeric isolators the most used device.

It has been experimentally and theoretically demonstrated, that an elastomeric isolator under axial load and lateral displacement has a reduction in its lateral stiffness and it is even possible to become unstable. Moreover, the axial and vertical stiffness of an isolator are reduced by the action of lateral displacement (Kelly et al., 2003). That situation corresponds to a coupling behaviour between axial load and lateral displacement, which is the reason why the overall behaviour is nonlinear.

The lateral-axial coupling occurs when the isolator is subjected to lateral displacement causing the cross section to rotate around a horizontal axis. The maximum rotation occurs in the middle section of the isolator when the top and bottom faces of the isolator remain horizontal. When the lateral displacement is to the right direction and the axial load is compression, a rotation is generated in the clockwise direction. However, when a tensile axial load is acting, the rotation direction can be reverse.

The rotation of the cross section causes that both axial and shear global loads have a projection on the mid-plane of each rubber sheet (plane located in the middle of the deformed rubber sheet's thickness). In other words, an horizontal and vertical component are generated in the local axis for both loads (see Figure 1). Due to the above described phenomenon, the horizontal component of the axial load increases the magnitude of local shear load and generates an increment of the lateral displacement. As a consequence of these two conditions, the lateral stiffness is reduced. Therefore, the local

displacement due to shear in each rubber sheet (u_{vn} in Figure 1, with axis X_n rotated in an angle α_n) has a vertical component, which is added to the vertical component of the local axial displacement (w_n in Figure 1, with axis Z_n rotated in an angle α_n). As a consequence of this situation, the vertical stiffness is reduced. The axial stiffness is always reduced when the lateral displacement is increased, under compressive or tensile axial loads. According Kelly (2003), “the mechanics of the isolator in tension are the mirror image of those for the isolator in compression”.

There are mathematical models that represent the lateral-axial coupling behaviour in a circular elastomeric isolator. However, these models characterize only the overall behaviour, which means that the model is able to globally predict the relationship between the axial and shear load, and between the vertical and horizontal displacement of the isolator, and it is unable to represent the stress-strain effect that occurs within each rubber sheet.

The objective of this research is to propose a nonlinear model that considers the lateral-axial interaction between loads and displacements within a circular multilayer elastomeric isolators. This model, in addition to characterizing the overall behaviour of the isolator, is also able to predict the internal stress-strain phenomena occurring within any rubber sheets of the isolator.

2 NON-LINEAR MODEL APPROACH

2.1 Equilibrium in a single rubber sheet

The basic hypothesis considered for this model is that rubber is a linear elastic material capable of achieving high levels of strain. However, since the thickness of each rubber sheet t_r is much smaller than its radius R , it can be assumed that the resulting force acting on the plane and the force perpendicular to the plane of the rubber sheet have negligible interaction. Therefore, it is necessary to know the response of a thin rubber sheet under load in their local axes: perpendicular to the mid-plane (Z_n) and parallel to the mid-plane (X_n), which is shown graphically in Figure 1.

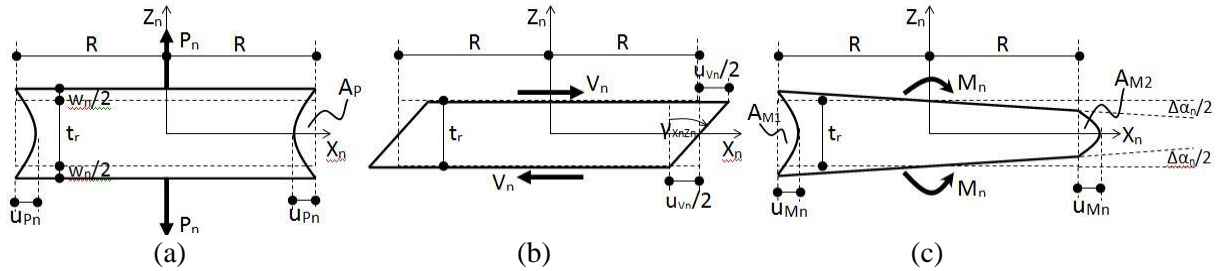


Figure 1. Axial load, shear load and bending moment acting individually in a single rubber sheet in its local axes, with the corresponding parameters of loads and associated displacements.

The mathematical relations between decoupled global loads acting on the isolator and the corresponding displacements, strains and stress, are well known because they arise from the differential equations that rule the rubber behaviour, which has been considered incompressible.

The load versus displacement mathematical relations and those used to obtain the maximum strain and stress in a deformed rubber sheet under uncoupled local loads (see Figure 1), come from the partial differential equation that governs the behaviour of this phenomenon.

The equation for pure local axial load is:

$$w_n = \frac{t_r}{6GAS^2} P_n \quad (1)$$

The equation that represents pure local shear load is:

$$u_{vn} = \frac{t_r}{GA} V_n \quad (2)$$

For the case of pure local bending moment, the equation is:

$$\Delta\alpha_n = \frac{t_r}{2GIS^2} M_n \quad (3)$$

where G is the shear modulus of rubber, A is the cross section area, S is the shape factor, I is the second moment of area (inertia) of the cross section and the other variables involved in those equations are shown in Figure 1.

The magnitude of maximum normal stress and strain are given by:

$$\sigma_{trac}^{max} = GS^2 \max \left\{ \frac{12}{t_r} w_n, \frac{8}{t_r} w_n + \frac{8S}{\sqrt{3}} \Delta\alpha_n, \frac{8}{t_r} w_n - \frac{8S}{\sqrt{3}} \Delta\alpha_n, 0 \right\} \quad (4)$$

$$\sigma_{com}^{max} = GS^2 \min \left\{ \frac{12}{t_r} w_n, \frac{8}{t_r} w_n + \frac{8S}{\sqrt{3}} \Delta\alpha_n, \frac{8}{t_r} w_n - \frac{8S}{\sqrt{3}} \Delta\alpha_n, 0 \right\} \quad (5)$$

$$\varepsilon_{trac}^{max} = \max \left\{ \frac{1}{t_r} w_n - \frac{R}{t_r} \Delta\alpha_n, \frac{1}{t_r} w_n + \frac{R}{t_r} \Delta\alpha_n, 0 \right\} \quad (6)$$

$$\varepsilon_{com}^{max} = \min \left\{ \frac{1}{t_r} w_n - \frac{R}{t_r} \Delta\alpha_n, \frac{1}{t_r} w_n + \frac{R}{t_r} \Delta\alpha_n, 0 \right\} \quad (7)$$

The magnitude of maximum absolute shear stress and strain is given by:

$$\tau^{max} = \max \left\{ \left| \frac{6GS}{t_r} w_n + 6GS^2 \Delta\alpha_n + \frac{G}{t_r} u_n \right|, \left| \frac{6GS}{t_r} w_n - 6GS^2 \Delta\alpha_n + \frac{G}{t_r} u_n \right| \right\} \quad (8)$$

$$\gamma^{max} = \frac{1}{G} \tau^{max} \quad (9)$$

2.2 Definition of the model

The model considers that the steel sheets are non-deformable. They have only translation and rotation like a rigid body and the deformation is concentrated in the rubber sheets (Figure 2). Each rubber sheet provides stiffness associated to local shear “ k_h ” (parallel to the deformed mid-plane of the rubber sheet), local axial load stiffness “ k_v ” (perpendicular to the deformed mid-plane of the rubber sheet), and bending moment stiffness “ k_a ” on local axis Y_n , perpendicular to the shear and axial local axis (axis X_n and Z_n in Figure 1).

The behaviour of the isolator system as a whole, is not linear, since the lateral displacement is large. This causes the rubber sheets to rotate, making the overall forces acting on the isolator to have components on both local axes of each rubber sheet, therefore producing the load interaction.

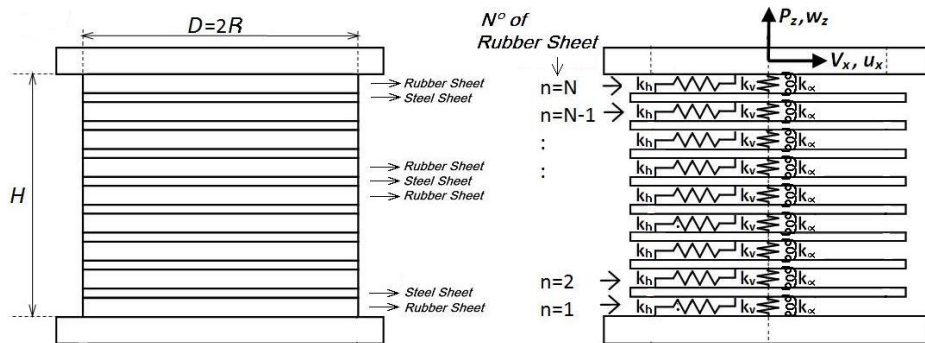


Figure 2. Multiple spring model (MSM), 3 springs per rubber sheet on isolator, to characterize the behaviour of coupled axial and shear loading. Consider that both, top and bottom of the isolator can not rotate.

2.3 Load versus displacement relationship

The rigid body rotation “ α_n ”, of the mid-plane of the n-th rubber sheet, due to applied loads, imposes a kinematic transformation for local displacements u_{Vn} , w_n , and $\Delta\alpha_n$ in local axes X_n , Z_n , which become the displacement variations, Δu_x^n and Δw_z^n , between bottom centroid of area of the n-th rubber sheet and top centroid of area of steel sheet immediately above the n-th rubber sheet, referred to global axes X , Z , which is given by:

$$\begin{bmatrix} \Delta u_x^n \\ \Delta w_z^n \end{bmatrix} = \begin{bmatrix} \cos(\alpha_n) & \sin(\alpha_n) \\ -\sin(\alpha_n) & \cos(\alpha_n) \end{bmatrix} \cdot \begin{bmatrix} u_{Vn} \\ w_n \end{bmatrix} + \begin{bmatrix} t_r \sin(\alpha_n) + t_s \sin(\tilde{\alpha}_n) \\ t_r \cos(\alpha_n) - t_r + t_s \cos(\tilde{\alpha}_n) - t_s \end{bmatrix} \quad (10)$$

where α_n is the rotation (clockwise positive direction) of the deformed mid-plane of n-th rubber sheet with thickness t_r , and $\tilde{\alpha}_n$ is the rotation of the steel sheet with thickness t_s , located above that rubber sheet.

The fundamental hypothesis proposed in this paper, is that the model displacement components of the n-th rubber sheet in their local axes, u_{Vn} and w_n are directly related to local loads, V_n and P_n , and the mathematical relation is given by the following decoupled linear equation:

$$\begin{bmatrix} u_{Vn} \\ w_n \end{bmatrix} = \frac{t_r}{6GAS^2} \begin{bmatrix} 6S^2 & 0 \\ 0 & 1 \end{bmatrix} \cdot \begin{bmatrix} V_n \\ P_n \end{bmatrix} \quad (11)$$

where the local loads and displacements are shown in Figure 1.

Local loads are related with global loads by a kinematic transformation, opposite to that represented by eq. 11.

$$\begin{bmatrix} V_n \\ P_n \end{bmatrix} = \begin{bmatrix} \cos(\alpha_n) & -\sin(\alpha_n) \\ \sin(\alpha_n) & \cos(\alpha_n) \end{bmatrix} \cdot \begin{bmatrix} V_x \\ P_z \end{bmatrix} \quad (12)$$

Adding the accumulated contributions of displacement in each rubber sheet and steel sheet due to global loads, and rotating that to the global axes X and Z using eq. 10 combined with eqs. 11 and 12, the overall load-displacement equation is obtained:

$$\begin{bmatrix} u_x \\ w_z \end{bmatrix} = \frac{t_r}{GA} \left[\begin{array}{cc} \sum_{n=1}^N \cos^2(\alpha_n) + \frac{1}{6S^2} \sin^2(\alpha_n) & -\left(1 - \frac{1}{6S^2}\right) \sum_{n=1}^N \cos(\alpha_n) \sin(\alpha_n) \\ -\left(1 - \frac{1}{6S^2}\right) \sum_{n=1}^N \cos(\alpha_n) \sin(\alpha_n) & \sum_{n=1}^N \left(\frac{1}{6S^2} \cos^2(\alpha_n) + \sin^2(\alpha_n)\right) \end{array} \right] \begin{bmatrix} V_x \\ P_z \end{bmatrix} \\ + \begin{bmatrix} \sum_{n=1}^N \sin(\alpha_n) & \sum_{n=1}^{N-1} \sin(\tilde{\alpha}_n) \\ \sum_{n=1}^N (\cos(\alpha_n) - 1) & \sum_{n=1}^{N-1} (\cos(\tilde{\alpha}_n) - 1) \end{bmatrix} \begin{bmatrix} t_r \\ t_s \end{bmatrix} \quad (13)$$

2.4 Solving the Nonlinear System

The nonlinear system of equations (eq. 13) appears to be indeterminate, because it has the redundant variables α_n and $\tilde{\alpha}_n$. However, these variables are related to the inner bending moment at the mid-plane of each rubber sheet, which is associated with an increase of rotation $\Delta\alpha_n$ (eq. 3).

Adding the increments of rotation, we have the absolute rotation of the mid-plane of the n-th rubber sheet and the rotation of the steel sheet above the n-th rubber sheet, which are:

$$\alpha_n = \frac{1}{2} \Delta\alpha_n + \sum_{k=1}^{n-1} \Delta\alpha_k \quad (14)$$

$$\tilde{\alpha}_n = \sum_{k=1}^n \Delta\alpha_k \quad (15)$$

where $\Delta\alpha_k$ is the increase in rotation developed in the k-th rubber sheet, which is related to the internal bending moment (eq. 3), evaluated at the level of the mid-plane of that rubber sheet. This bending moment “ M_k ” is given by:

$$M_k = M_y(z^{(k)}) \approx \frac{1}{2H} (V_x(H + w_z) - P_z u_x)(H - (2k - 1)t_r - 2(k - 1)t_s) \quad (16)$$

Using eqs. 16 and 3, it is possible to calculate the increasing of rotation, $\Delta\alpha_n$, for $n=1$ to N (where N is the number of rubber sheets), knowing the global loads (V_x and P_z) and an initial approximation of the global displacements (u_x and w_z). Before that, knowing the value of $\Delta\alpha_n$, it is possible to calculate the rotations α_n and $\tilde{\alpha}_n$. Then, it is possible to re-estimate the global displacement and re-calculate the bending moment M_n , the increasing of rotation $\Delta\alpha_n$ in the n-th rubber sheet, and the total rotations α_n and $\tilde{\alpha}_n$, for $n=1 \dots N$. The calculation process is repeated iteratively until achieving convergence. As an initial approximation of the global displacements to start the iterative process, the linear relationship given by eq. 13 can be considered, assuming $\alpha_n = \tilde{\alpha}_n = 0$, for $n=1$ to N .

3 MODEL RESULTS

The model was used to obtain the response of a single circular multilayer elastomeric isolator, with radius $R=30$ cm, rubber sheets thickness $t_r=12$ mm, steel sheets thickness $t_s=3$ mm, 40 rubber sheets (N), a shape factor $S=12.5$ and shear modulus of $G=7.5$ kg/cm² for the rubber.

All global loads are shown as a proportion of the critical buckling load P_{cr} , obtained from the model of two springs (Kelly, 2003).

3.1 Load versus displacement curves

Model results are shown in terms of load versus displacement curves (Figures 3 to 5, left side) and stiffness reduction factor curves (Figures 3 to 5, right side). The results obtained using the proposed model were compared with those obtained using the two springs model (Koh and Kelly, 1987; Kelly, 2003; Ryan et al., 2005).

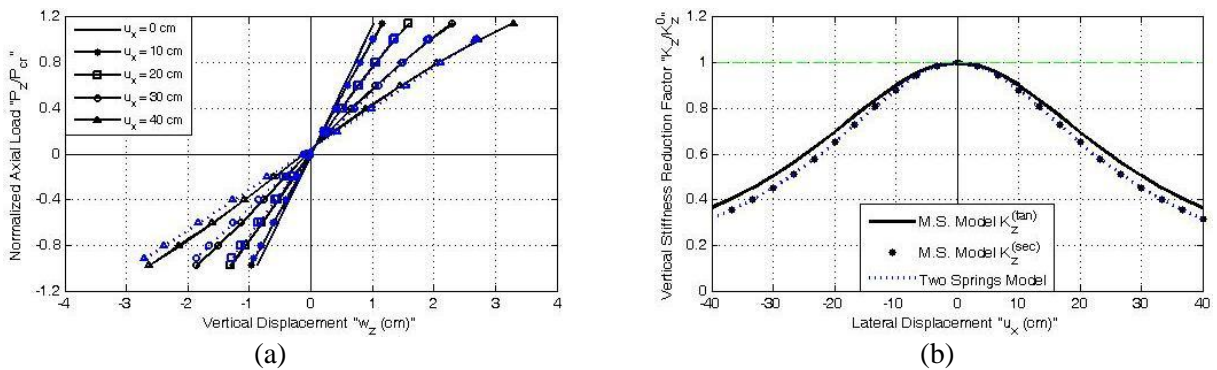


Figure 3. (a) Axial Load versus vertical displacement as a function of lateral displacement (compression $P_z < 0$ and traction $P_z > 0$). (b) Vertical stiffness reduction factor as a function of lateral displacement.

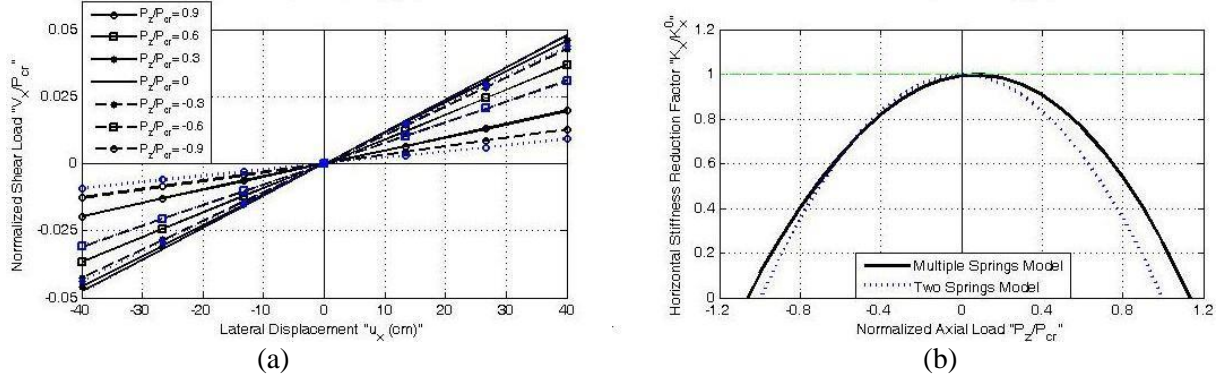


Figure 4. (a) Shear load versus lateral displacement as a function of “ P_z/P_{cr} ”. (b) Horizontal stiffness reduction factor as a function of of “ P_z/P_{cr} ” (compression $P_z < 0$ and traction $P_z > 0$).

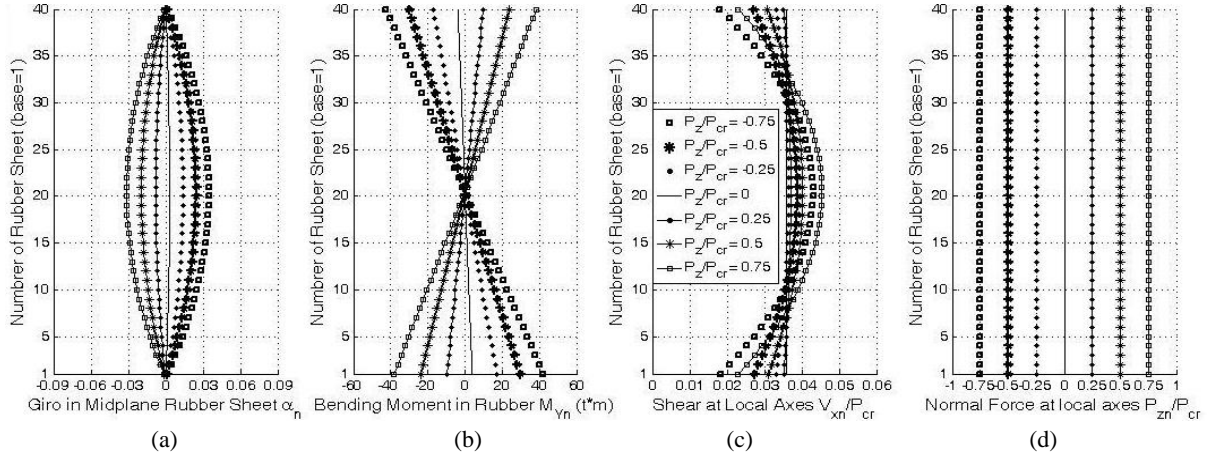


Figure 5. (a) Rotation in mid-plane of each rubber sheet, (b) Bending moment, (c) Normalized shear load in local axis X_n , (d) Normalized axial load in local axis Z_n . It was considered horizontal displacement $u_{Xn}=30$ cm.

The reduction pattern of vertical stiffness with the increase of lateral displacement is virtually identical between the proposed model (secant stiffness) and the two springs model (Figure 3b). Moreover, the pattern of reduction in lateral stiffness with the increase of axial load shows no significant differences in compression (Figure 4b, left side). In this case, both curves (proposed model and two springs model) are close by, and the critical buckling load reached in the proposed model is approximately 5% larger than that of the two springs model. However, in tension (Figure 4b, right side), the critical buckling load differs from the two springs model in approximately 15 %, and it also shows an asymmetry relative to the axial load.

There is a slight increase of lateral stiffness due to a small tensile load (Figure 4b), which is explained because lateral displacement generates a rotation of rubber sheets that is opposite to that generated for a tensile load. When the tensile load is not enough to revert the rotation due to lateral displacement, the projection of tensile load on the rubber sheets' local axis X_n is opposite to the global shear projected on X_n , therefore, these are subtracted, generating an increase of stiffness. However, when the tensile load is large enough to revert the rotation due to lateral displacement, the projection of tensile load on rubber sheets' local axis X_n is added to the projection of the global shear on X_n , which generate a reduction of stiffness.

3.2 Maximum Stress and Strains

The stress and strain in many points inside rubber, along the entire isolator, were obtained for many combinations of axial load and lateral displacement. After analysing all rubber layers, it was determined that the maximum stress and strain is always developed in the bottom and top rubber sheets. The maximum strain and stress generated in the lower rubber sheet are shown in Figures 6 to 8.

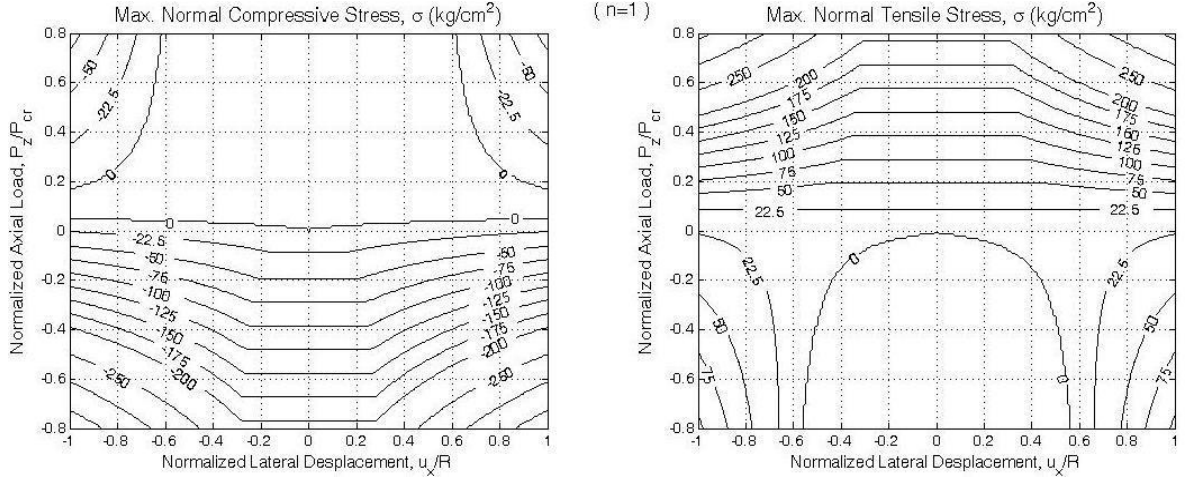


Figure 6. Maximum normal stress, as a function of axial load and lateral displacement.

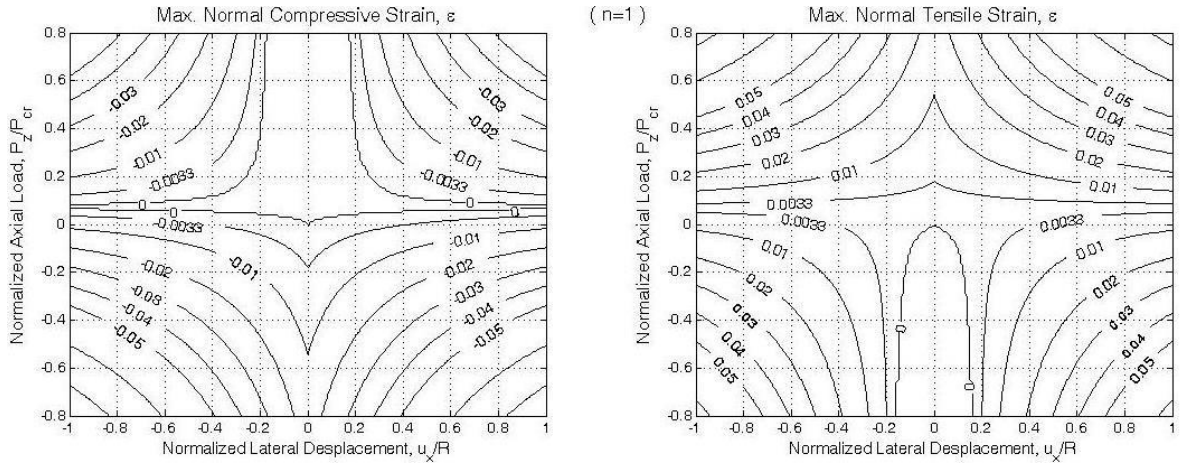


Figure 7. Maximum normal strain, as a function of axial load and lateral displacement.

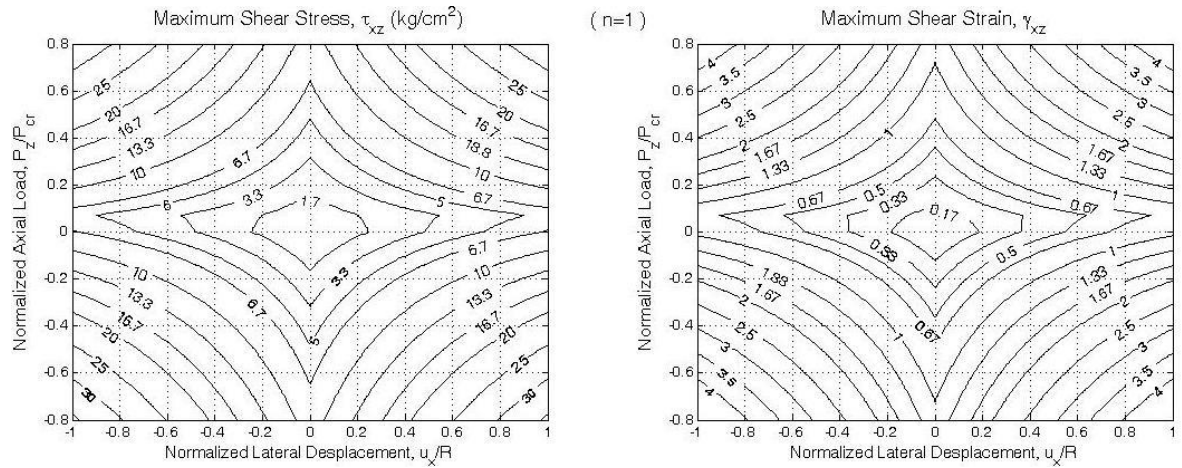


Figure 8. Maximum shear stress and strain, as a function of axial load and lateral displacement.

The tensile stress of cavitation in the rubber is about three times the shear modulus (Gent, 1990), which corresponds to 22.5 kg/cm² for the example shown in Figures 3 to 8. In Figure 6 the contour-curve associated with this stress corresponds to a plateau that is only reached at a load of about 10% of the critical buckling load P_{cr} (taken from the two springs model (Kelly, 2003)), even in the case of large lateral displacements ($u_x = \pm R$). In contrast, the same stress in compression is reached at a global

compressive load of 10% of the P_{cr} only for $|u_x| < 0.17R$; whereas for $u_x = \pm R$ the same stress can be reached without requiring axial load. This suggests that it is possible to generate a not insignificant level of axial tensile load (10% of the P_{cr}) in the elastomeric isolator, and not necessarily exceeds the cavitation tension.

The normal strain for which cavitation theoretically occurs in rubber, is given by $\varepsilon_c = 1/(2S^2)$ (Kelly, 2003), which corresponds to $\varepsilon_c = 0.0032$ for the case shown in Figures 3 to 8. In Figure 7, it is observed that even with large lateral displacements ($u_x = \pm R$), normal tensile strain could be smaller than the cavitation, at least in a limited range of axial loads (3% to 5% of P_{cr}). Also, there is a safe range in which no cavitation occurs ($|u_x| \leq 0.4R$ and $P_z \leq 0.1P_{cr}$).

The above is an advantage that would allow the design of rubber isolators under the action of significant levels of axial tensile load (10% of the P_{cr}), without exceeding the stress and strain of rubber cavitation, for a not negligible lateral displacement range, which is $|u_x| \leq 0.4R$ for the example shown in this study. This is particularly important in high-rise buildings, where the rocking could produce tensile stress in rubber isolators, because the isolators require a large radius due to their large weight. Therefore, it is highly probable that the safety range will not be exceeded.

In many experimental studies of isolators under tensile load required by the US seismic code, when uplift on an isolator is predicted by analysis, it was observed that none of the tested isolators failed by cavitation (Kelly, 2003). In contradiction to the theoretical calculations that predicts deformation that exceeded cavitation conditions. The model introduced in this paper provides analytical evidence that suggests the possibility of using elastomeric isolation under to tensile loads in a safe manner.

4 CONCLUSIONS

The results of this research suggest the possibility of using elastomeric seismic isolation safely in a range of axial load ($|u_x| \leq 0.4R$ and $P_z \leq 0.1P_{cr}$) that is not negligible in comparison with the critical buckling load, even with lateral displacement of comparable magnitude to the radius.

Unlike what is usually considered regarding the behaviour of an elastomeric isolator in tension and compression as being the mirror image of each other (Kelly, 2003), this model makes a difference that can be substantial, particularly when the axial load is small ($P_z < 0.2P_{cr}$) which is common in real designs (Ryan et al 2005).

The buckling load is theoretically higher under tensile loads than under compression, whereas the behaviour of the isolator is non-simetric with respect the axial load.

REFERENCES

- Chen, S.C. Tian, X.K. Yan, W.M. & K. Kim, S. 2013. Modeling and analysis of laminated rubber bearings under axial tensile loading. *Materials and Structures*.
- Forcellini, D. & Kelly, J.M. 2013. The Analysis of the Large Deformation Stability of Elastomeric Bearings. *Journal of Engineering Mechanics*, 10.1061/(ASCE)EM.1943-7889.0000729.
- Gent, 1964. Elastic estabily of rubber compression springs. *Journals of Mechanics Engineering*, SCI. A.N.
- Gent, 1990. Cavitation in rubber: A cautionary tale. *American Chemical Society*. A.N.
- Han, X. Warn, G.P. & Kasalanati, A 2013. Dynamic Stability Testing of Isolation Systems Composed of Elastomeric Bearings and Implications for Design, *Structures Congress*, American Society of Civil Engineers, 2013: pp. 2140-2150.
- He, W. Liu, W. Yang, Q. & Feng, D. 2012. Nonlinear Rotation and Shear Stiffness Theory and Experiment Research on Rubber Isolators. *Journal of Engineering Mechanics: (ASCE)*.
- Kelly, J.M. 2003. Tension buckling in multilayer elastomeric bearing. *Journals of Engineering Mechanics ASCE*.
- Koh, C. & Kelly, J.M. 1987. Effects of axial loads on alastomeric isolator bearings.
- Liu, W. He, W. Feng, D. & Yang, Q. 2009. Vertical Stiffness and Deformation Analysis Models of Rubber Isolators in Compression and Compression-Shear States. *Journal of Engineering Mechanics*, 135(9), 945–952.

- Nagarajaiah, S. & Ferrell, K. 1999. Stability of Elastomeric Seismic Isolation Bearings, *Journal of Structural Engineering*.
- Ravari, A.K. Othman, I.B. Ibrahim, Z.B. & Ab-Malek, K. 2012. P- Δ and End Rotation Effects on the Influence of Mechanical Properties of Elastomeric Isolation Bearings: *Journal of Structural Engineering: (ASCE)* 138(6), 669–675, 2012.
- Ryan, K.L. Kelly, J.M. & Chopra, A.K. 2004. Experimental observation of axial-load effects in isolators bearings, *World Conference on Earthquake Engineering*. Paper No 1707, Canadian association for Earthquake Engineering.
- Ryan, K.L. Kelly, J.M. Chopra, A.K. 2005. Nonlinear model for lead-rubber bearing including axial-load effects, *Journals of Engineering Mechanics ASCE*.
- Ryan, K.L. & Chopra, A.K. 2005. Estimating the seismic response of base-isolated building torsion, rocking, and axial load effects.
- Yang, Q. Liu, W. He, W. & Feng, D. 2010. "Tensile Stiffness and Deformation Model of Rubber Isolators in Tension and Tension-Shear States." *J. Eng. Mech.*, 136(4), 429–437.